

# SCIENTIFIC REPORTS



OPEN

## 1-Methyl-D-tryptophan Reduces Tumor CD133<sup>+</sup> cells, Wnt/ $\beta$ -catenin and NF- $\kappa$ Bp65 while Enhances Lymphocytes NF- $\kappa$ B2, STAT3, and STAT4 Pathways in Murine Pancreatic Adenocarcinoma

Murad Alahdal<sup>1,2</sup>, Yun Xing<sup>1</sup>, Tingting Tang<sup>1</sup> & Jin Liang<sup>1</sup>

1-Methyl-D-tryptophan (1-MT) is extensively utilized in preclinical trials to deplete indoleamine 2,3-dioxygenase (IDO) activity and kynurenine pathway. Since IDO related signaling pathways aren't well understood, some clinical reports affirmed IDO inhibiting therapeutic significance. Therefore, we did use direct tumor autologous antigens vaccination and 1-MT without chemotherapy to explore biological mechanisms and immunomodulations of 1-MT that motivate antitumor responses. However, DCs antigen-uptake capability, anti-tumor efficiency, intra-tumor and intracellular cytokines were assessed. Besides, CD133<sup>+</sup> cells viability and tumor biomarkers were investigated. Splenocytes responses and their signaling pathways such TLRs 2 to 9, NF- $\kappa$ B1-2, Wnt/ $\beta$ -catenin and TGF- $\beta$  were dissected. Results evinced that a regimen of 1-MT and TAAs significantly reduced CSC CD133<sup>+</sup> viability inside tumor microenvironment, besides increasing tumor cells necrosis and apoptosis. Expression of TGF- $\beta$ , IDO, RANTES, and PDL-1 was also significantly reduced. Interestingly, 1-MT enhanced lymphocytes TLR2, TLR7, TLR8, and TLR9 pathways. It motivated lymphocytes' NF- $\kappa$ B2, STAT3, and STAT4 pathways, while reduced tumors' NF- $\kappa$ Bp65 and Wnt/ $\beta$ -catenin signaling pathways. We found that periphery and intra-tumor Treg cells were significantly decreased. In conclusion, depletion of indoleamine 2,3-dioxygenase activity evidenced IDO relation with tumor stem cells proliferation pathways. Furthermore, 1-MT supports immunotherapeutic vaccines susceptibility and tumor specific targeting by reducing tumorigenesis signaling pathways.

Indoleamine 2,3-Dioxygenase checkpoint inhibitors are extensively concerned in the current clinical trials towards several tumor types<sup>1-3</sup>. There are plenty of IDO checkpoint inhibitors, but 1-Methyl-D-tryptophan (1-MT) recently showed promising efficient. It's a racemic substance blocks kynurenine pathway, and classified as a main responsible of tryptophan and catabolic kynurenine depletion, which selectively impairs T cells proliferation and survival, because T lymphocytes are sensitive to loss tryptophan amino acid<sup>4,5</sup>. Normally, IDO protects maternal tolerance of pregnant's fetus from T cell responses to MHC-mismatched heterograft<sup>6,7</sup>. New evidences suggest that, IDO becomes highly activated during cancer development<sup>8</sup>. It supports tumor cells escape eradication by immune system<sup>8-10</sup>. Clinical reports concluded that IDO overexpression could polarize APCs to enhance tumor proliferation. Moreover, transfection of tumor cells by IDO gene showed an immunosuppressive activity<sup>11,12</sup>, which glimpses IDOs' succoring role toward tumor tolerance. The investigation of IDO expression in tumor cells showed that, IDO overexpression into tumor cells is controlled by *Bin1* (tumor suppressor gene), while this gene becomes disabled during tumor development for unknown reasons yet<sup>9</sup>. Therefore, several

<sup>1</sup>State Key Laboratory of Natural Medicines, Jiangsu Key Laboratory of Drug Ability of Biopharmaceuticals, Jiangsu Key Laboratory of Drug Screening, School of life science and Technology, China Pharmaceutical University, Nanjing, China. <sup>2</sup>Medical Laboratory department, Faculty of Medicine and Health Sciences, Hodeidah University, Al Hudaydah, Yemen. Correspondence and requests for materials should be addressed to J.L. (email: [ljestemcell@cpu.edu.cn](mailto:ljestemcell@cpu.edu.cn))

projects consider IDO work motifs, which could explain clear working itinerary of IDO related pathways to help identification of critical therapeutic target. Because, a lot of human aggressive cancers such as pancreatic, colorectal, lung, ovarian, prostatic, cervical, gastric, head, etc. demonstrated high expression of this enzyme or tryptophan metabolic derivatives<sup>13,14</sup> during tumor development stage.

Furthermore, a study of IDO-tryptophan catabolism and immune mechanisms in the tumor microenvironment is cloudy and needs more understanding<sup>2</sup>, subsequent studies represented that IDO has multiple immunological functions. It promotes different signaling pathways to suppress T-cell responses, and enhancing Treg cells<sup>15,16</sup>. Collecting all these details together, we find that IDO knockout or inhibition without chemotherapy applications could represent IDO biological signaling pathways in tumor cells and lymphocytes. Nevertheless, IDO relation with immune cells is also complicated and needs deep understanding. It mainly produced from Mesenchymal stromal cells, endothelial cells, fibroblasts, and myeloid-derived antigen-presenting cells<sup>17,18</sup>. Recent reports conducted that mature and immature DCs rather than plasmacytoid DCs could overexpressed IDO in some metastatic cancers<sup>19,20</sup>. Thus signaling pathways involved IDO during tumor related immunomodulations are versatile and poorly understood. Moon Yong *et al.*<sup>21</sup> revealed that IDO provokes tryptophan shortage, which leads to mechanistic target of rapamycin inhibition (mTORC1) and general control non-depressible 2 (GCN2) activation, that causes anergy of Th1. Meanwhile, bioactive kynurenine pathway stimulates Aryl hydrocarbon receptor (AHR), resulting in promotion of Treg differentiation<sup>21</sup>. Moreover, It was thought that a mechanism of tryptophan degradation happened by base-catalyzed abstraction<sup>22</sup>, while recently was concluded that this mechanism involves formation of a transient ferryl<sup>23</sup>. Whereas, Li, Fang xuan *et al.*<sup>24</sup> summarized that IDO1 could induces most of immune cells participations. Particularly APCs and cancer related cells through NF- $\kappa$ B canonical and non-canonical, Jak/STAT pathways, PKC and TGF- $\beta$  signaling pathways<sup>25</sup>.

Therefore, we blocked IDO activity by using 1-Methyl-D-tryptophan, and used a biological vaccine (tumor autologous antigens) to explore clear evidences regarding virtual work mechanisms and pathways ascribed to IDO activity, without chemotherapy that could confuse results interpretation, because of its harmful side effects<sup>26</sup>. We considered pancreatic adenocarcinoma model in the mice, because recently it's one of the most aggressive cancers in the world, which showed high rates of IDO overexpression associated tumor aggressiveness<sup>27,28</sup>.

## Results

**TL efficiently activates DCs maturation and T cell during 24 hours.** The analysis of DCs tumor antigens (TL) uptake potential showed that DCs significantly pulsed in response to tumor lysate in comparison to PBS. It presented high maturation responses; CD40<sup>+</sup>CD80<sup>+</sup> cells that were gated from CD11c gate represented 74.7% under the impact of TL in comparison to PBS 21.9% (Fig. 1A). Meanwhile, MHCII, CD40 and CD80 genes expression showed significant increasing in comparison to PBS (Fig. 1B); these findings suggested that DCs effectively recognized tumor antigens and efficiently presented to T cell. On the other hand, the determination of optimal time point to activate T cell kinetic and polarization toward tumor antigens showed that accumulation of intracellular INF- $\gamma$  in CD3<sup>+</sup>CD4<sup>+</sup> cells was increased during 9 hours to reveal 3.15%, but a significant level of INF- $\gamma$  was detected after 24 hours 6.35% as represented in (Fig. 1C); whereas the accumulation of INF- $\gamma$  in CD3<sup>+</sup>CD8<sup>+</sup> cells was also showed significant raising after 24 hours 7.65% as seen in (Fig. 1D). Later, we confirmed these results by analysis *INF- $\gamma$* <sup>+</sup> gene expression in splenocytes by qRT-PCR, which showed a significant expression of *INF- $\gamma$* <sup>+</sup> after 24 hours of incubation (Fig. 1E).

**1-MT and Tumor lysate inhibit tumorigenesis and elicit tumor inflammatory necrosis.** Subsequently, *in vivo* tumorigenesis progression dynamics were significantly inhibited under 1-MT+TL, and 1-MT+DCs-TL regimens effect. We noted that tumor growth of 1-MT, 1-MT+TL, and 1-MT+DCs-TL groups was significantly reduced in comparison to PBS group (2.16 mm<sup>3</sup>/1.30 g, 1.68 mm<sup>3</sup>/1.12 g, 2.14 mm<sup>3</sup>/1.27 g, and 2.5 mm<sup>3</sup>/2.51 g) respectively (Fig. 2A,C,D). Moreover, the survival rate of 1-Methyl-D-tryptophan treated groups were significantly improved (88days/38.64%, 78days/30.77%) respectively in comparison to PBS (54days) as showed in (Fig. 2B). Furthermore, the analysis of tumor histology showed that 1-MT and 1-MT+TL significantly elicited inflammations and tumor necrosis inside tumor tissue more than 1-MT+DCs-TL (Fig. 2E(a,b,c)). These results indicated that 1-MT effectively enhanced the performance of TL vaccine to elicit lymphocytes responses against tumor. Also, pathologist report described destruction of tumor stromal fibers in groups treated by 1-MT which illustrated an interesting impact of 1-MT on tumor fibrosis.

**1-MT and 1-MT+TL effectively reduces tumor fibrosis.** Tumor fibrosis was critically assessed by using Picro-Sirius red staining technique (PSR) to determine tumor collagen fibers area under 1-MT effect; stained sections showed that 1-MT, 1-MT+TL and 1-MT+DCs-TL groups significantly reduced collagen fibers distribution around tumor tissue in comparison to PBS, it measured 1.77%, 0.99%, 2.69%, and 12.38% respectively (Fig. 2F(a,b,c)). So, collagen fibers deposition were decreased in tumors treated 1-MT. Collagen folding and deposition of PBS group 12.38% ((Fig. 2F(g)) was found higher than 1-MT treated groups that interestingly indicate a high impact of 1-MT on tumor fibrosis.

**1-MT significantly activates caspase-3 and apoptosis.** The impact of 1-MT on tumor cell apoptosis was investigated by testing an immune reactivity of cleaved caspase-3 pathways of 1-MT treated and untreated groups. We found that 1-MT extremely increased caspase3 reactivity in treated tumors (Fig. 2G(a,b,c)), while other groups showed no apoptotic reactions (Fig. 2G(d,e,f,g)). This indicates that 1-MT has a potential role to enhance tumor cell destruction by activating apoptotic signaling pathways.

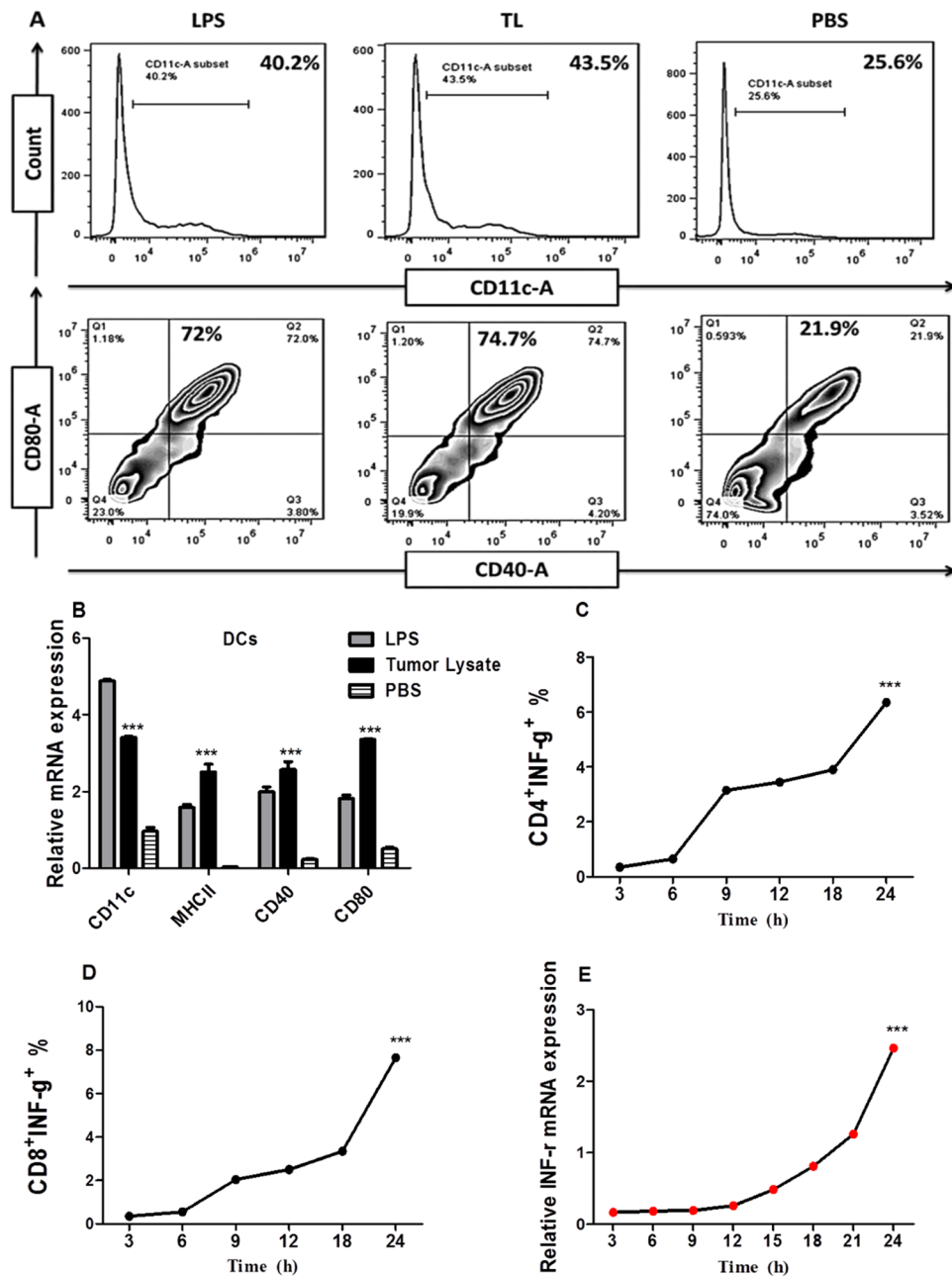


**Figure 1.** DCs loaded tumor lysate (TL) were tested by Flowcytometer and RT-qPCR to check DCs capability to uptake tumor antigens and present them to Th1 cells. It showed that MHCII, CD40, and CD80 were significantly stimulated by tumor antigens (TL) in comparison to positive and negative controls (A,B). This is proved that DCs successfully uptake tumor antigens and proceeded presenting potency. Besides that, determination of specific time point to activate Th1 and CTL cells responses by tumor lysate was performed by Flowcytometer interval 3 hours; it showed a highest INF- $\gamma$ <sup>+</sup> accumulation at 24 hour, as showed in (C), CD4<sup>+</sup>INF- $\gamma$ <sup>+</sup> gated from CD3<sup>+</sup> significantly raised after 9, 12, and 18 hours, but the highest response showed at 24 hours of incubation. While CD8<sup>+</sup> INF- $\gamma$ <sup>+</sup> activation significantly rose at 18 hours and the highest response was noted at 24 hours of incubation (D), these results were confirmed by RT-qPCR to determine a relative INF- $\gamma$  mRNA expression after activation of splenocytes by (TL = 20 ug/ml). Results showed that high response started at 18 hours to reach a highest at 24 hours (E). The statistical significant differences were represented from at least three independent experiments, \*\*\*P < 0.001.

**1-MT enhances TILs and significantly reduces CSC.** Further analysis of tumor tissues and microenvironment lymphocytes showed that 1-MT significantly enhanced Th1 cells CD3<sup>+</sup>CD4<sup>+</sup>CD25<sup>-</sup> alone and with TL/DC-TL (23.3%, 19.2%, and 21.6%) respectively in comparison to PBS (13.4%). Meanwhile, it significantly reduced Treg cells CD4<sup>+</sup>CD25<sup>+</sup>Foxp3<sup>+</sup> in the tumor microenvironment in comparison to PBS group (6.13%, 2.32%, 5%,

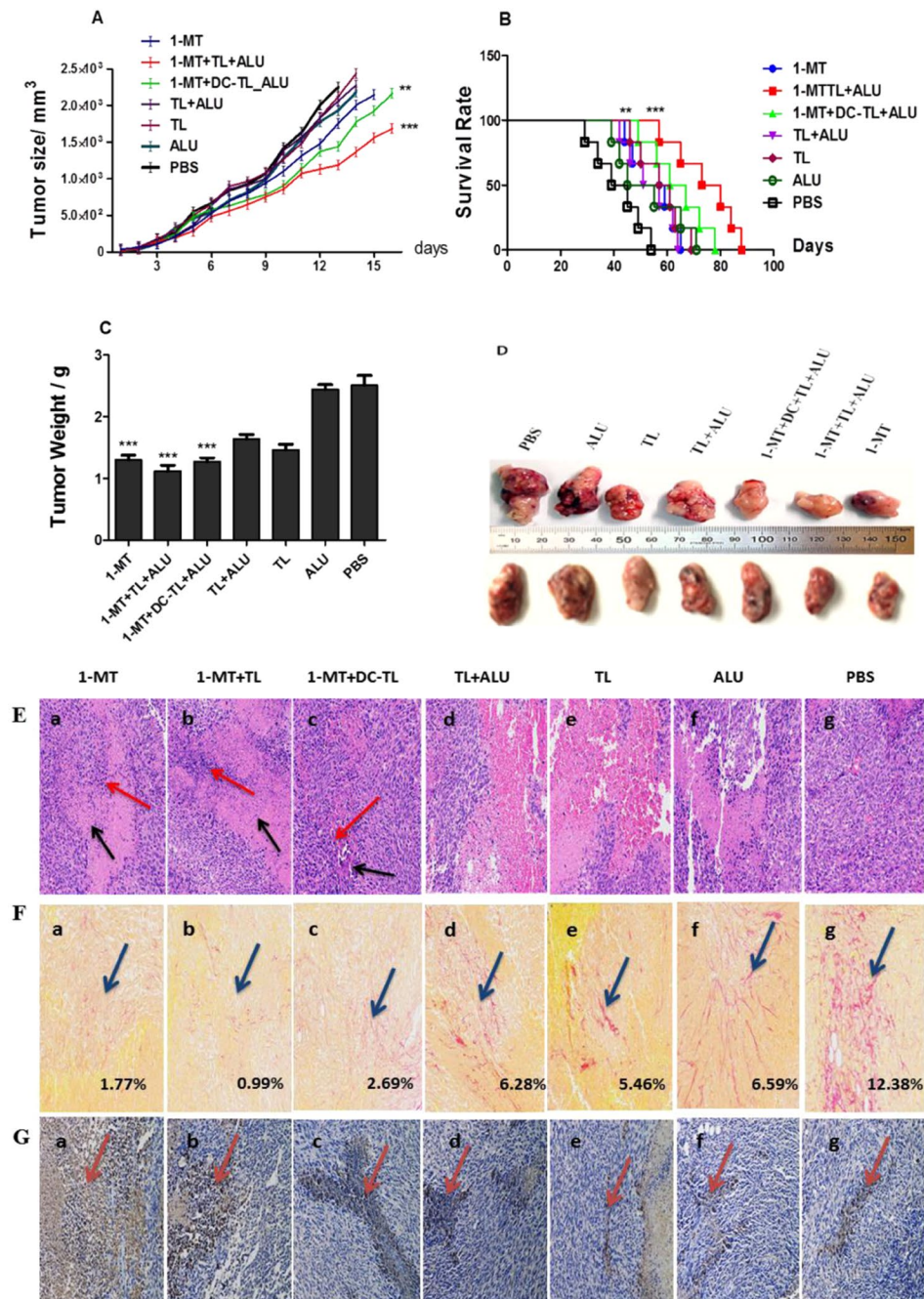


**Figure 2.** An *in vivo* evaluation of 1-MT+TL/DCs-TL vaccination efficacy in C57BL/6 black mice challenged Pan02 tumor model showed that 1-MT and 1-MT+TL/DCs-TL significantly reduced tumor size 2.144 cm<sup>3</sup>, 1.686 cm<sup>3</sup>, 2.166 cm<sup>3</sup> respectively (A), tumor volume and weight also significantly reduced (C,D). Besides survival rate of 1-MT+TL/1-MT+DCs-TL treated groups was significantly improved (B), 38.64%, and 30.77% respectively in comparison with PBS group. Further Haematoxylin and Eosin (H&E) staining showed that, mice treated by 1-MT and 1-MT+TL (E.a,b) significantly represented many focal necrosis accompanied with more inflammatory infiltrating cells (black arrow for focal necrosis, and red arrow for inflammatory cells). Meanwhile 1-MT+DC-TL treated group (E.c) showed small tumor necrosis and few numbers of inflammatory infiltrating cells. Other tested groups (E.d,e,f and g) represented a small focal necrosis inside tumor tissue and a little number of inflammatory cells. The assessment of tumor fibrosis showed that 1-MT, 1-MT+TL, and 1-MT+DCs-TL groups extremely decreased collagen deposition folding rate in treated tumors as shown around pointed area (F.a,b,c), while other groups showed high collagen fibers (F.d,e,f,g). Besides that 1-MT treated groups showed significant immune reactivity of cleavage caspase3 pathway (G.a,b,c) that indicated promoting of tumor apoptosis. While other untreated groups showed no significant apoptotic reactions (G.d,e,f,g). These results indicated that administration of 1-Methyl-D-tryptophan and TAA vaccine destroyed tumor stromal and fibrosis, while it promoted significant apoptosis and cell death, which is very interesting observation. \*\*\*( $P < 0.0001$ ), and \*\*( $P < 0.001$ ).

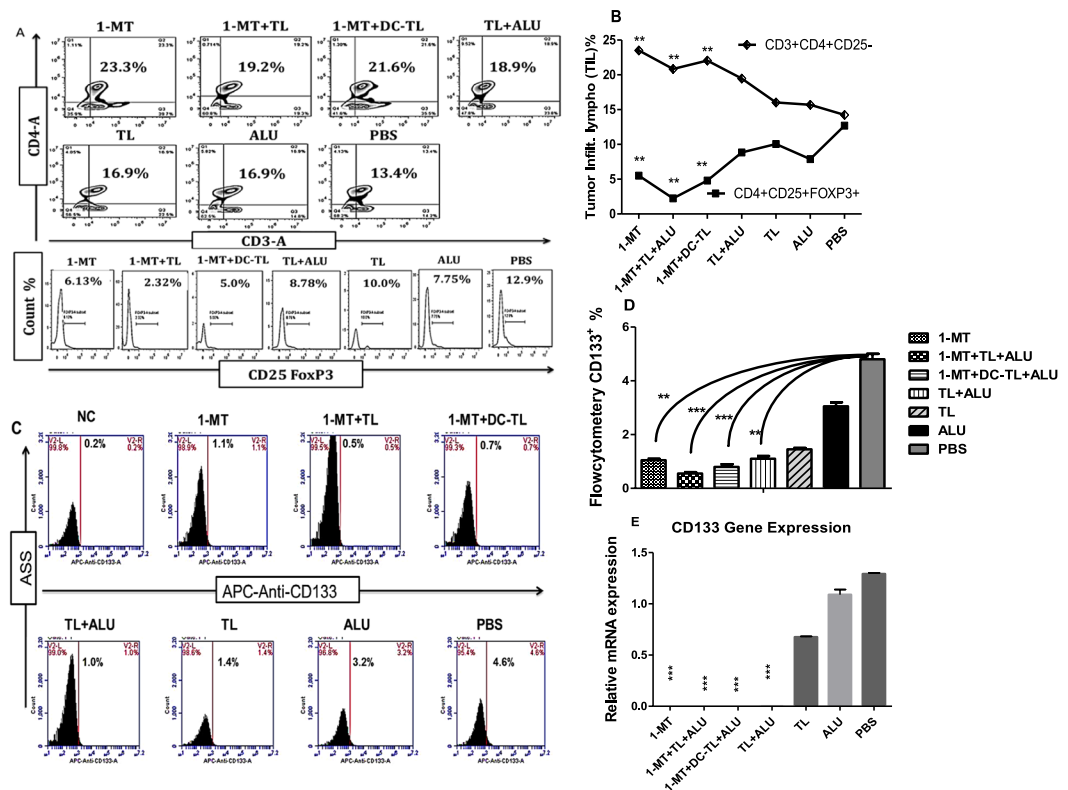


**Figure 3.** Analysis of tumor infiltrating lymphocytes by Flowcytometer showed that a population of Th1 cells ( $CD3^+CD4^+CD25^-$ ) was significantly increased inside tumors of 1-MT, 1-MT+TL and 1-MT+DC-TL treated groups in comparison to PBS (A,B). Meanwhile, Treg<sup>+</sup> cells ( $CD25^+FOXP3^+$ ) were significantly reduced in comparison to PBS. Cancer stem cells (CSC)  $CD133^+$  viability in tumor microenvironments of all tested groups showed that 1-MT, 1-MT+TL and 1-MT+DC-TL extremely reduced  $CD133^+$  viability in comparison to PBS group (C,D), as well as the analysis of relative mRNA showed that  $CD133$  gene expression was significantly declined in 1-MT+TL and 1-MT+DC-TL treated groups in comparison to PBS group (E). These results indicated that 1-MT significantly enhanced TL to elicit immunosurveillance that recognizes and effectively reduces CSC prognosis, which inhibits tumor growth and tumorigenesis. \*\*\*( $P < 0.0001$ ), and \*\*( $P < 0.001$ ).

and 12.9%) respectively (Fig. 3A,B). Whereas a screening of  $CD133^+$  cells in tumor microenvironment showed that 1-MT, 1-MT+TL, and 1-MT+DCs-TL were significantly reduced a population of  $CD133^+$  cells in the tumor microenvironment in comparison to PBS (1.0%, 0.5%, 0.7%, and 4.6%) respectively (Fig. 3C,D). These results were ensured by determination of relative  $CD133$  mRNA gene expression among total tumor cells RNA. We found that expression of mRNA was significantly reduced by 1-MT in comparison to PBS (Fig. 3E).

**1-MT reduces regulatory pathways and enhances tumor inflammatory modulations.** Consequently, relative mRNA assessment of intra-tumor cytokines revealed that 1-MT significantly reduced CCL5 (RANTES) and TGF- $\beta$ , besides inhibition of IDO enzyme in comparison to PBS as showed in (Fig. 4B,E,F). Nevertheless, 1-MT significantly enhanced inflammatory cytokines CCL2 (MCP-1), CCL7 (MCP-3), and CCL20 (MIP3A) as presented in (Fig. 4A,C and D). The analysis of intra-tumor signaling pathways showed that 1-MT and tumor lysate significantly reduced PDL-1, NF- $\kappa$ B2, TRAF1,  $\beta$ -Catenin, and IKK $\beta$  as presented in (Fig. 4G,H,I,J and L). While, IKK $\alpha$  mediator was significantly activated (Fig. 4K); these results indicated an impact of 1-MT on tumorigenesis pathways such as NF- $\kappa$ B, Wnt/ $\beta$ -catenin, and TGF- $\beta$  signaling pathways. 1-Methyl-D-tryptophan significantly inhibits most of tumor regulatory pathways which do enhance accelerating tumor proliferation and tolerance. These evidences were confirmed by western blot.

**1-MT and tumor lysate inhibits tumor regulatory pathways.** Total protein contents of tumor tissues were obtained to evaluate signaling pathways expression; total extracted proteins were loaded by protein loading buffer (PLF) (Blossom, China) for 10 min at 100 °C. Then 5  $\mu$ g/ml of each protein samples was tested by western blot with Page Ruler Protein marker (Thermo scientific, USA) to test TGF- $\beta$ , PDL-1, NF- $\kappa$ B2, IDO,  $CD133$  and  $\beta$ -catenin in comparison to GAPDH positive control. Results showed that 1-MT, tumor lysate, and DCs-pulsed tumor lysate were significantly reduced expression of TGF- $\beta$ , PDL-1, NF- $\kappa$ B2, IDO, and  $\beta$ -catenin in comparison to PBS as showed in (Fig. 5A,B). These outputs accumulated more evidences of 1-MT related mechanisms in tumor cells, which confirmed results of genes expression profile screening of intracellular signaling pathways. It interpreted why 1-MT could modulate various humoral and cellular responses.

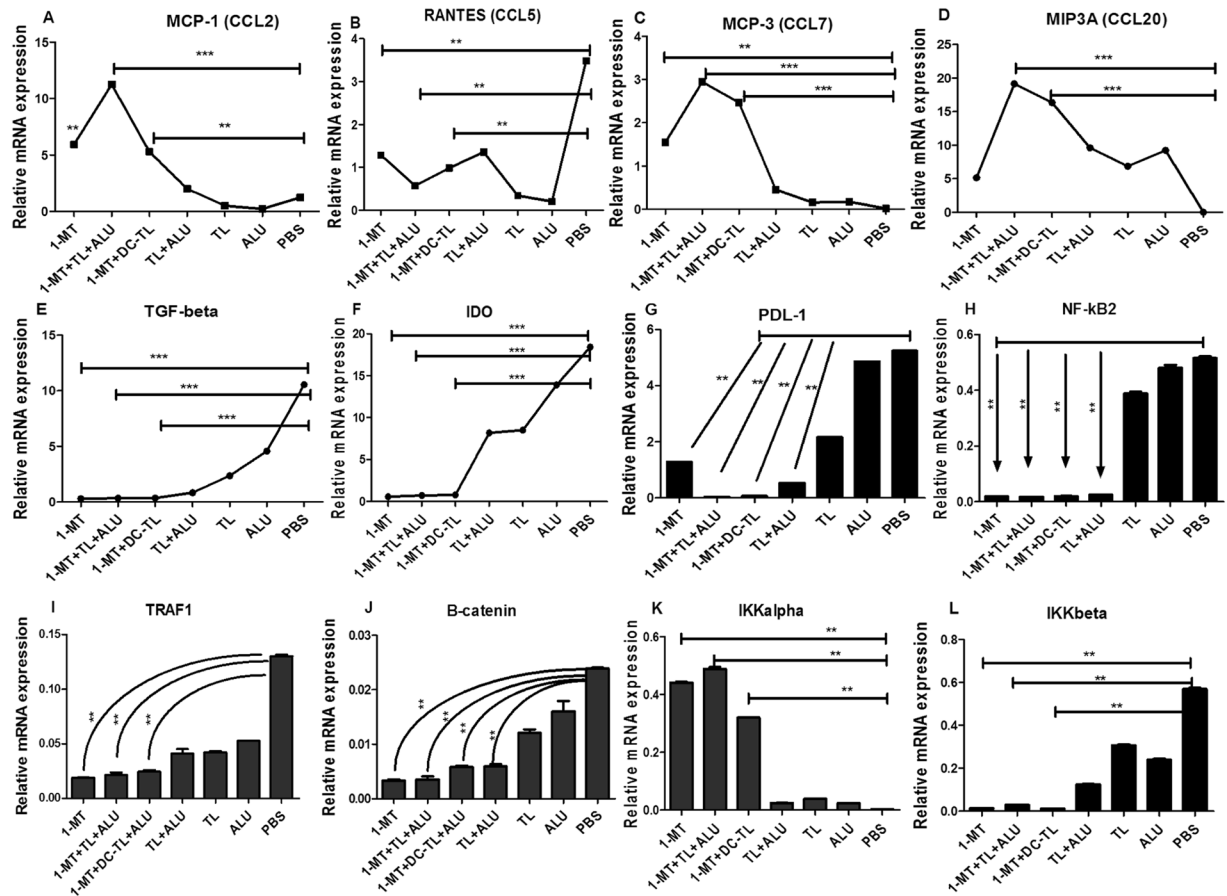


**Figure 4.** Genetic expression profile of intra-tumor microenvironment cytokines and pathways showed that MCP1, MCP3, and MIP3A were significantly enhanced by 1-MT, 1-MT+TL and 1-MT+DC-TL regimens in comparison to PBS group (A,C and D). Meanwhile, RANTES, TGF- $\beta$ , IDO, and PDL-1 were significantly reduced in comparison to PBS group (B,E,F and G). Further tumor genetic screening showed that NF- $\kappa$ B2, and  $\beta$ -Catenin pathways were interestingly reduced (H,J) by 1-MT, 1-MT+TL and 1-MT+DC-TL regimens, also TRAF1, and IKK $\beta$  mediators were significantly inhibited (I,L), while IKK $\alpha$  was significantly induced (K). These findings clearly evidenced that 1-MT effectively enhanced inflammatory immunomodulations inside tumor microenvironment in response to TL/DCs-TL vaccines, it also reduced tumorigenesis enhancers that lead to prevent tumor homing Treg cells as showed in the Fig. 2, which ensured a breakdown of tumor immunotolerance, and recognition of tumor cells by immune surveillance. The statistical significant differences were represented from at least three independent experiments, \*\*\*P < 0.001 and \*\* (P < 0.001).

#### Immunofluorescence imaging evidences blocking of NF- $\kappa$ Bp65 signaling pathway by 1-MT.

Laser imaging of intracellular NF- $\kappa$ Bp65 expression of Pan02 tumor cell line which was exposed to 1-MT or non exposed to 1-MT showed that IDO depletion effectively inhibited NF- $\kappa$ Bp65 signaling pathway (Fig. 6), that ensured a role of IDO in NF- $\kappa$ B pathway activation in response to regulatory polarization, the inhibiting of this pathway by 1-MT leads to breakdown tumor tolerance which facilitate modulation of immune responses inside tumor microenvironment.

**1-MT and TL or DCs-TL promotes splenocytes inflammatory responses.** The analysis of CD4<sup>+</sup> and CD8<sup>+</sup> T cells' *ex vivo* kinetics of all immunized groups according to the determined time point (24 hs) showed that 1-MT itself significantly enhanced high accumulation of INF- $\gamma$  in CD4<sup>+</sup> cells rather than its efficacy with TL stimulation and also DCs-TL in comparison to PBS group as shown in (Fig. 7A), As well as, CTL (CD8<sup>+</sup>) cells were also showed significant increasing of INF- $\gamma$  in response to TL and DCs-TL stimulation in comparison to PBS (Fig. 7B). On the other hand, genes expression of regulatory and inflammatory mediators illustrated that 1-MT elicited increasing of IL-12, 1L-6, and IL-4 expression (Fig. 7C,D,E), while it declined TGF- $\beta$ , and IL-10 expression (Fig. 7F,G). These results suggested that 1-MT enhanced Th1 CD4<sup>+</sup>, and CTL CD8<sup>+</sup> activation, to initiate proinflammatory immune mediators, while it reduced Treg cells expanding which ascribed to decline of regulatory mediators.

**1-MT promotes splenocytes' TLRs signaling pathways in response to TL/DCs-TL.** Further splenocytes genes expression profile screening under 1-MT treated groups demonstrated that 1-MT significantly promoted splenocytes' TLR2, 7, 8, and 9 in comparison to PBS, while TL, DCs-TL also promoted these pathways,

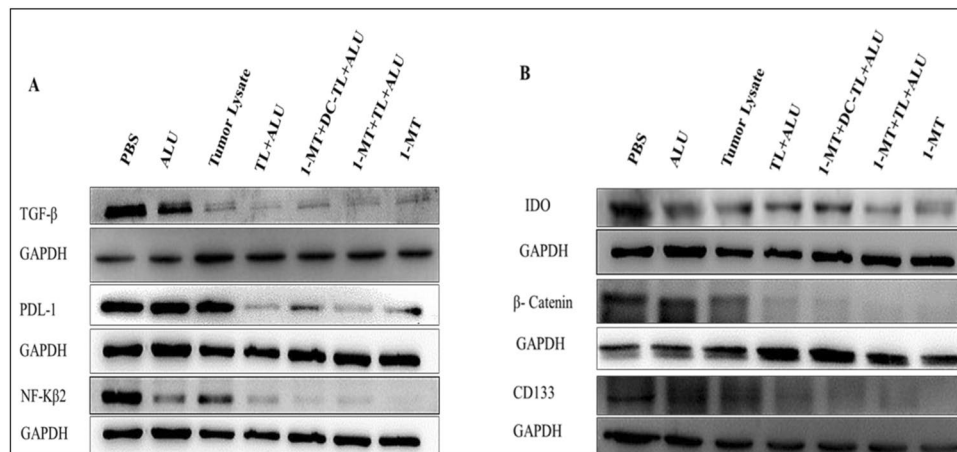


**Figure 5.** Analysis of tumor microenvironments' mediators, markers and signaling pathways under the effect of 1-MT-TL/DCs-TL regimens by western blot presented that TGF- $\beta$ , PDL-1, and NF- $\kappa$ 2 were significantly inhibited in comparison to PBS (A). Meanwhile, IDO,  $\beta$ -catenin, and CD133 showed significant reduction under the effect of 1-MT, 1-MT+TL, and 1-MT+DCs-TL in comparison to PBS (B). These results clearly evidenced that 1-MT extremely prohibited main tumor growth, progression, and immune escaping pathways, which activates immune surveillance restore and recruits cellular and humoral immune responses triggering tumor tissues.

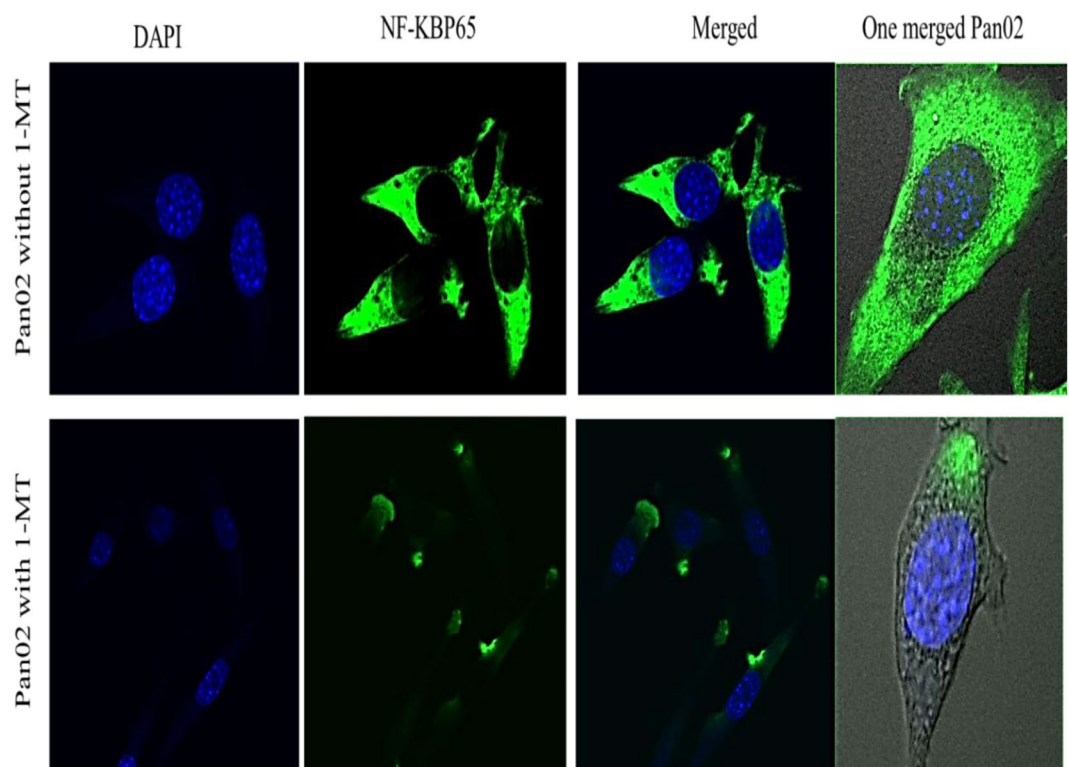


**Figure 6.** Investigation of NF- $\kappa$ 3p65 pathway activity of Pan02 cell line under the effect of 1-MT *in vitro* illustrated that 1-MT effectively inhibited NF- $\kappa$ 3p65 in the tumor cells which proved that 1-Methyl-D-tryptophan efficiently depletes tumorigenesis activity and forbid tumor immunosuppressive pathways.

but pathways expression was accelerated by 1-MT (Fig. 8A,E,F and G). Meanwhile, other tested TLRs showed no significant responses towards TL, DCs-TL or 1-MT (Fig. 8B,C and D). Furthermore, deep investigation of intracellular pathways showed that 1-MT significantly enhanced an expression of Myd88, TRAF6, IRAK4, STAT3, STAT4, NF- $\kappa$ 3, AP-1, and IKK $\alpha$ , while an expression of IKK3, and NF- $\kappa$ 31 was significantly declined (Fig. 8H,I). These results clearly evidenced a role played by IDO towards T cells proinflammatory initiations, which mainly enhances immune regulatory and tumor tolerance through inhibition of immune surveillance functions. Here, 1-MT interestingly facilitated provoking of T lymphocytes immune responses towards tumor antigens.

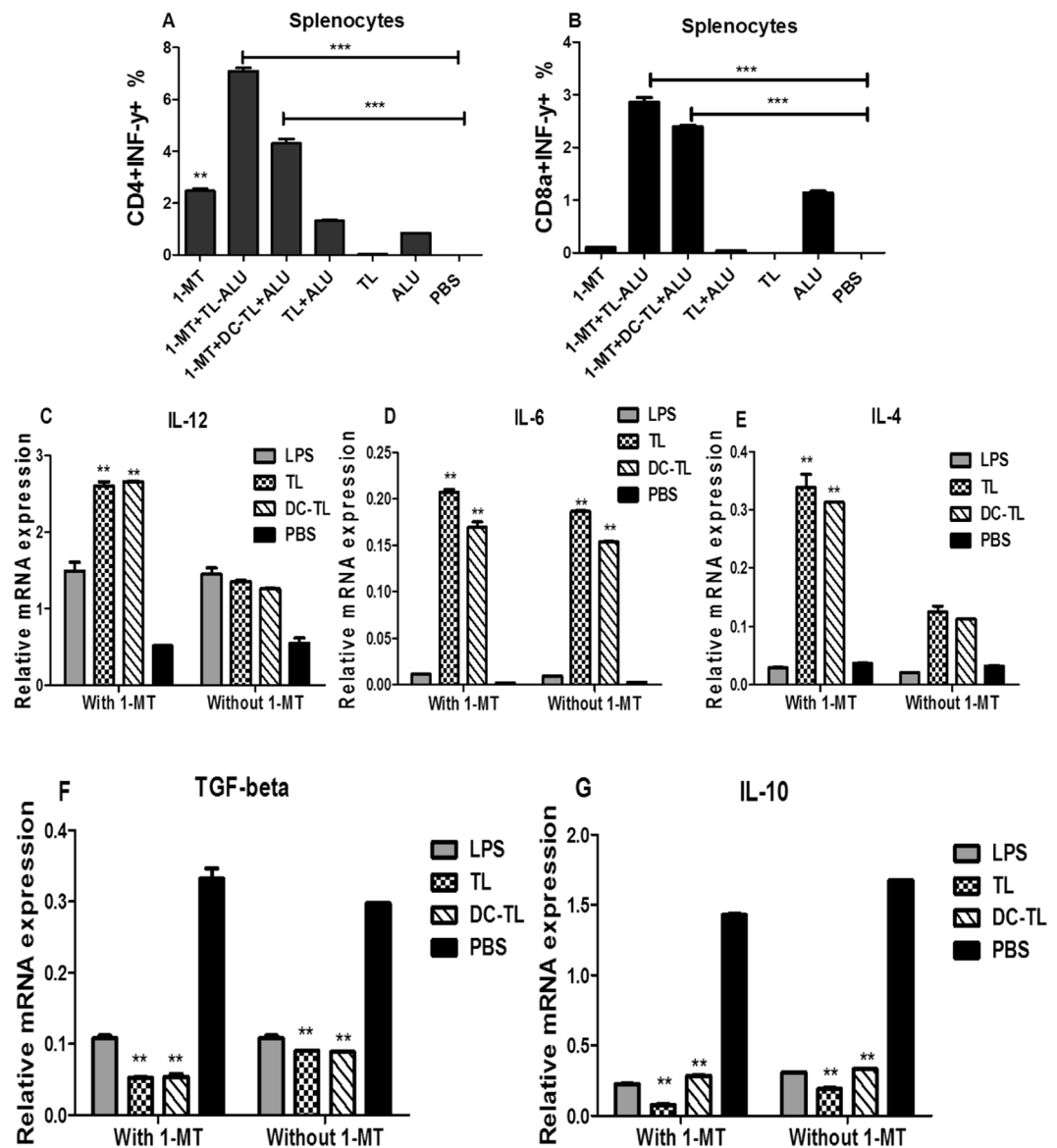


**Figure 7.** *Ex vivo* lymphocytic kinetic responses of 1-MT treated mice showed that 1-MT significantly elicited inflammatory responses, it enhanced CD4<sup>+</sup>INF-γ<sup>+</sup> and CTL INF-γ<sup>+</sup> accumulation within 24 hours of incubation (A,B). Besides, the analysis of inflammatory mediators' relative mRNA expression revealed that 1-MT significantly enhanced IL-12, IL-6, and IL-4 secretion in response to TL/DCs-TL antigens (C,D and E), while TGF-β and IL-10 were significantly reduced in comparison to PBS (F,G). These results accumulated more evidences confirming specific tumor targeting potential and inflammatory modulations. The statistical significant differences were represented from at least three independent experiments, \*\*\*P < 0.001 and \*\* (P < 0.001).

**Activation of periphery immune surveillance.** Confirmative immunological assessment of periphery immune pathways showed that Treg cells CD25<sup>+</sup>Foxp3<sup>+</sup> were significantly reduced in the periphery samples of mice treated by 1-MT and TL or DCs-TL in comparison to PBS (4.76%, 1.12%, 8.7%, and 21.7%) respectively (Fig. 9A and C). Meanwhile, CD3<sup>+</sup>CD4<sup>+</sup>CD25<sup>-</sup> cells were significantly increased in comparison to PBS (73.9%, 74.7%, 74.2%, and 27.8%) respectively (Fig. 9B). Then analysis of periphery cytokines showed that circulating IL-12 was significantly increased at 1-MT, 1-MT+TL, and 1-MT+DCs-TL treated groups in comparison to PBS (55.76, 85.17, 71.53, and 24.8 ng/L) respectively (Fig. 9E). Meanwhile, an investigation of circulating TGF-β showed that periphery TGF-β was significantly declined in mice treated 1-MT, 1-MT+TL, and 1-MT+DCs-TL in comparison to PBS group (0.97, 0.98, 1.26, and 7.90 pg/ml) respectively (Fig. 9D). These findings evidenced that humoral and cellular inflammatory responses were extremely modulated in 1-MT, 1-MT+TL, and 1-MT+DCs-TL treated groups, whereas regulatory mediators were significantly reduced which suggested that tumor tolerance would be broken down and tumor escaping from immunosurveillance would be inhibited.



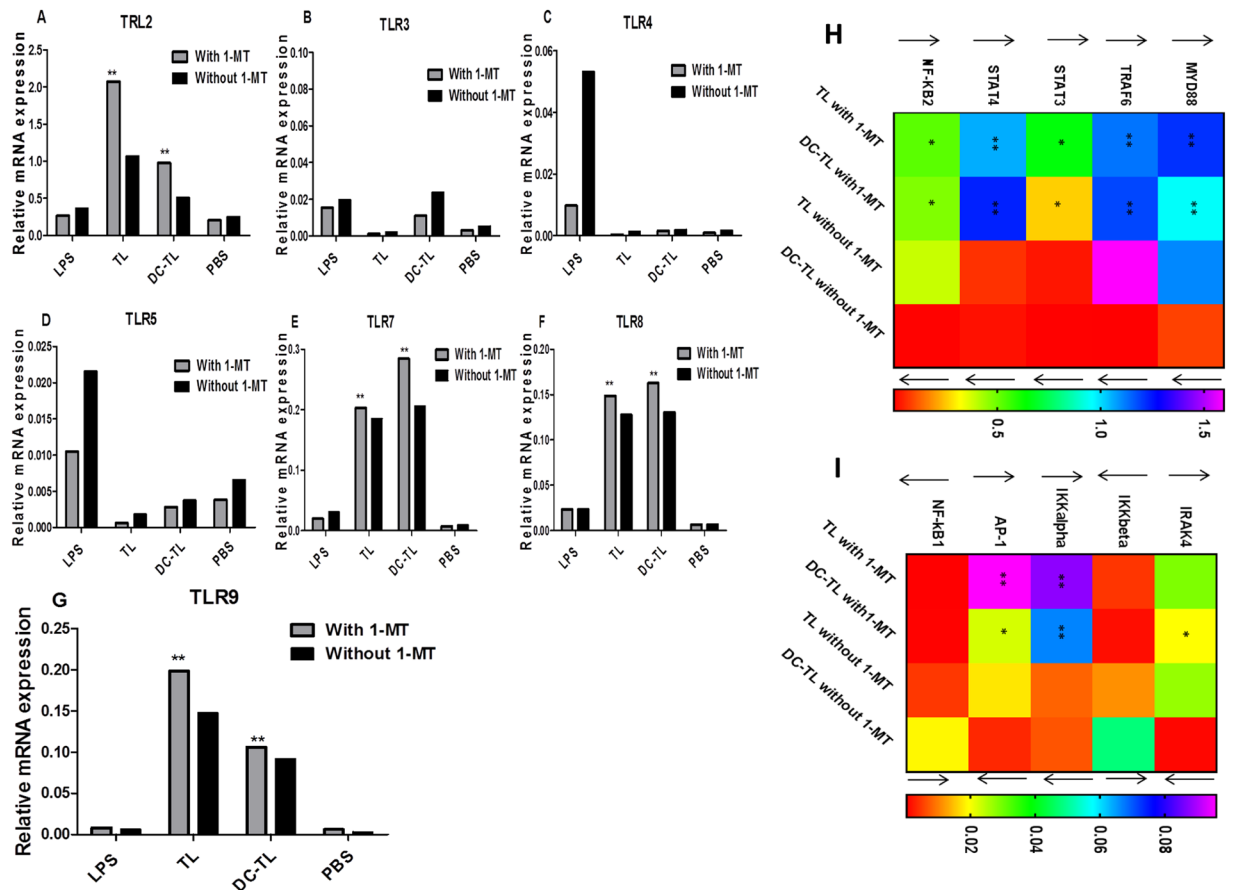


**Figure 8.** Gene expression profile of splenocytes' TLRs signaling pathways was determined. Results showed that 1-MT significantly provoked lymphocytic TLR2, TLR7, 8, and 9 in responses to TL/DCs-TL exposure (A,E,F and 9), while other investigated TLRs showed no responses for TL/DCs-TL effect (B,C and D). Further investigation of intracellular motifs expression profile represented that Myd88, TRAF6, STAT3, STAT4, IRAK4, IKK $\alpha$ , AP-1, and NF- $\kappa$ B2 mediators were significantly motivated under the effect of 1-MT in response to TL/DCs-TL exposure (H,I), while regulatory mediators IKK $\beta$  and NF- $\kappa$ B1 were significantly inhibited in comparison to cells without 1-MT. these results showed that 1-MT is the main responsible of immune inflammatory responses to TL/DCs-TL antigens elicitation, that showed no significant responses without 1-MT presence. The statistical significant differences were represented from at least three independent experiments, \*\*\* $P < 0.001$  and \*\*( $P < 0.001$ ).

## Discussion

It's well-known, that intracellular indoleamine-2,3-dioxygenase IDO by the depletion of tryptophan exerts an immunosuppressive pathways to induce tumor immune escaping<sup>21</sup>. Clinical trials (NCT02077881, NCT00567931) showed that combining IDO inhibitors such as 1-MT with other autologous antigens, chemotherapy, or itself could restore immune immunosurveillance performance<sup>9,29</sup>. To date many cancer regimens were tested, all of them showed limited clinical efficacy, because recruiting T cells against tumor isn't enough, it becomes functionally inactive when exposure to tumor microenvironment, which was ascribed to overexpression of IDO and regulatory mediators<sup>2,5,30</sup>. Meanwhile, signaling pathways that being orchestrated by IDO mechanisms in tumor microenvironment or myeloid cells are yet poorly understood<sup>21</sup>. Here, we investigated an efficient anti-tumor responses of TL/DCs-TL vaccination, which enhanced by 1-MT performance and its related signaling pathways to understand prognostic IDO work mechanisms related tumor growth, proliferation, and immunosuppressive pathways. We found that IDO mechanisms are complex, there are many signaling pathways mediated by this factor. Blockage of this enzyme enhanced significant humoral and cellular pathways responses to tumor lysate vaccine and/or DCs pulsed tumor lysate, besides significant improvements showed in clinical trials with chemotherapy used 1-MT checkpoint inhibitor<sup>21,31,32</sup>, which clearly evidenced that depletion of IDO activity instantly leads to increase therapeutic susceptibility. Interestingly, we didn't found documented information about the role of IDO inhibitor on CD133<sup>+</sup> cancer stem cells (CSC), while our results showed that 1-MT with/without tumor lysate vaccine significantly reduced CD133<sup>+</sup> cells viability in treated tumor tissues, which suggests that IDO motif role is orchestrated by CSC in the tumor microenvironment. Also, PDL-1 expression was significantly reduced under the effect of 1-MT in comparison to PBS group. This consequently led to inhibit tumorigenesis activities, which indicated that cancer stem cells mainly involve IDO pathways to develop tumorigenesis. As the analysis of

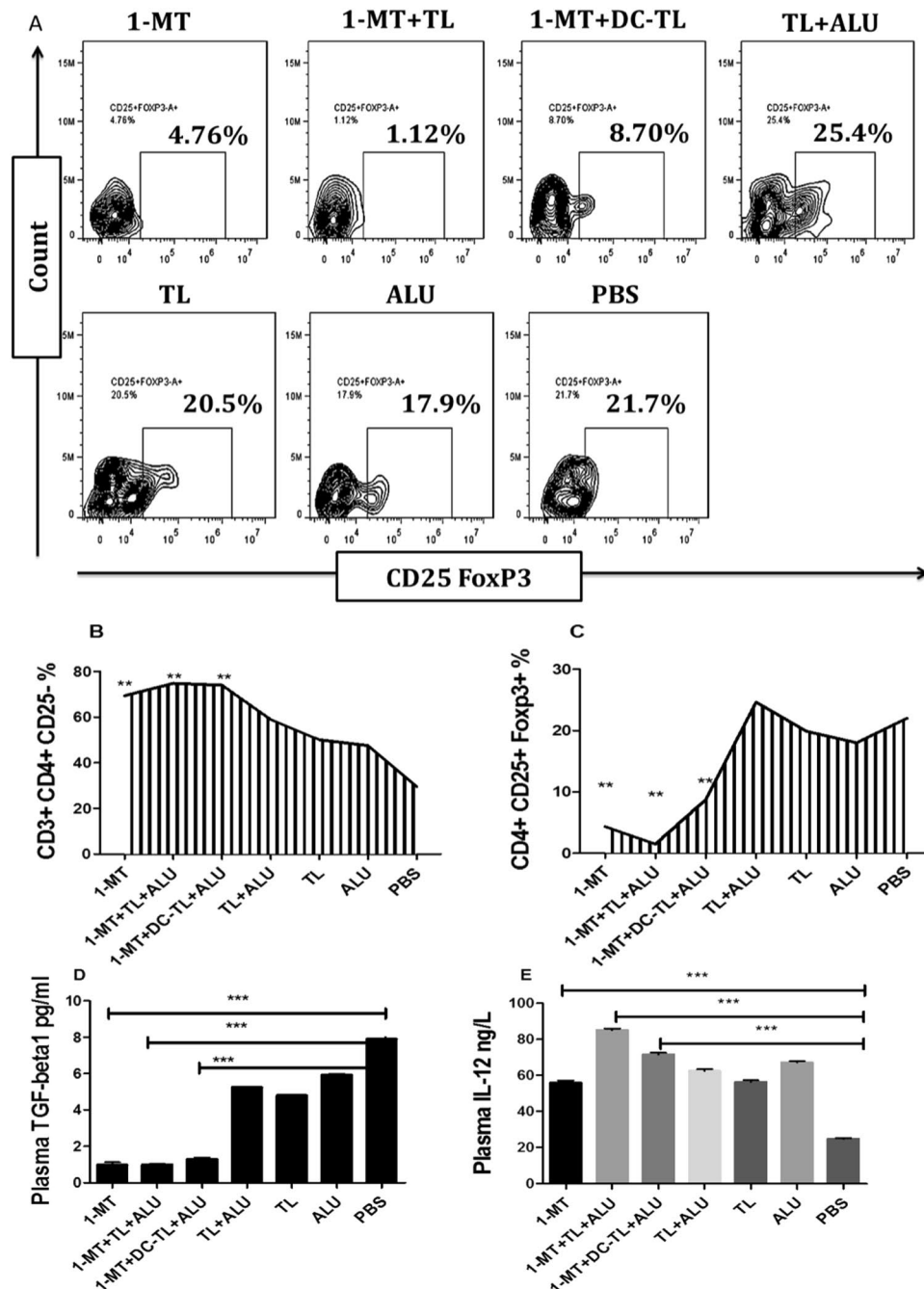


**Figure 9.** Periphery of cellular and humoral immunological responses of all mice groups illustrated that, administration of 1-MT, 1-MT+TL, and 1-MT+DCs-TL significantly reduced Treg cells population (CD4<sup>+</sup>CD25<sup>+</sup>FOXP3<sup>+</sup>) in comparison to PBS group (4.76%, 1.12%, 8.7%, and 21.7%) respectively (A and C), while CD4<sup>+</sup>CD25<sup>-</sup> cells were significantly increased in comparison to PBS (73.9%, 74.7%, 74.2%, and 27.8%) respectively (A,B). ELISA analysis of periphery cytokines showed that circulating TGF-β was significantly reduced in the mice immunized by 1-MT, 1-MT+TL, and 1-MT+DCs-TL (D), while analysis of IL-12 showed significant rising in comparison to PBS (E). This is proved that tumor immunosuppressive pathways were completely blocked, while immunosurveillance and inflammatory immunomodulations were efficiently activated. Statistical significant differences were represented from at least three independent experiments, \*\*\*P < 0.001 and \*\* (P < 0.001).

*in vivo* tumor apoptosis and tumor fibrosis under 1-MT effect showed that 1-MT significantly activates cleaved caspase3 and increased apoptotic potential, while it extremely reduced tumor fibrosis. These findings confirmed a role of IDO in tumor survival and progression, because knocking out IDO activity enhances tumor destruction and promotes tumor apoptosis that illustrates an impact of 1-MT on tumorigenesis pathways. This expresses a

significance of IDO blockage during tumor therapy. Furthermore, our results accumulated sequential evidences from splenocytes, DLN, and periphery that confirmed a significant promoting role of 1-MT for inflammatory responses and invasion of xenografted tumor models in groups vaccinated tumor lysate, and DCs pulsed TL in case of 1-MT administration, which were on the same line of several studies that investigated likely similar regimens<sup>33–36</sup>. In this study we found that 1-MT significantly reduces tumor cells IKK $\alpha$ , NF- $\kappa$ B2, and Wnt/ $\beta$ -catenin pathways, besides modulation of its regulatory cytokines in the tumor microenvironment, which significantly inhibited tumor growth and tumor immune escaping potency, that was on the same line of several previous studies<sup>37,38</sup>, but our findings showed that 1-MT significantly enhances IKK $\alpha$ , NF- $\kappa$ B2, STAT3, and STAT4 pathways of lymphocytes in response to TL/DCs-TL vaccination, which indicated that 1-MT activates intracellular signal transducer, in response to vaccination to induce tumor specific targeting, because activated DCs efficiently trigger presentation of tumor associated antigens to elicit specific tumor targeting. Because we found that TLR2, 7, 8, and 9 were significantly activated in the splenocytes of TL/DCs immunized mice during 1-MT addressing, which elucidated non-enzymatic activity of IDO engage tumorigenesis proceeds. These evidences apparently revealed that 1-MT completely forbids tumor tolerance pathways, which interprets the reduction of regulatory mediators and Treg cells in the tumor microenvironment and periphery analysis. These analyses represented a virtual anti-tumoral kinetics during vaccination period, which provided some biological evidences that could optimize solid tumor treatment strategies in the near future

## Conclusion

We conclude that, our results revealed that 1-MT has a potential to breakdown tumor tolerance and significantly releases immunosurveillance potential throughout depletion of kynurenine related pathways, besides activation of functional DCs and specific T cells to recognize tumor antigens and activate inflammatory modulations efficiently. These processes involve enzymatic and non-enzymatic mechanisms that need deep analysis of metabolic products pathways as a fundamental secret to identify specific motifs could lead to design high critical therapeutic strategies. However, tumor autologous antigens vaccine with 1-MT showed a significant therapeutic potential as an immunotherapeutic vaccine towards pancreatic adenocarcinoma in the murine models, which encourage this strategy implementation in human clinical trials.

## Materials and Methods

**Mice details and Ethical Issue.** Black females (20–25) g C57BL/6 mice were recruited from the Laboratory Animal Center of Yangzhou University. Experimental animals were housed in plastic cages under pathogen-free conditions. Experiments were performed in accordance with the National Institute of Health Guide for the Care and Use of Laboratory Animals, meanwhile it approved by the Institutional Animal Care and Use Committee of China Pharmaceutical University.

**Preparation of Tumor lysate (TL) and DCs loaded TL.** Pan02 cell line was utilized to prepare freeze-thawed tumor lysate, as described by W. Asavaroengchai *et al.*<sup>39</sup>. Then protein concentration of supernatant was determined by BCA protein assay kit (Beyotime, China), according to the manufacturer instructions. However, 20 ng/ml of tumor lysate was introduced to ( $1 \times 10^6$ ) bone marrow dendritic cells (DCs) for 24 hours, in comparison to 1 ng/ml LPS and PBS. Later, pulsed DCs were stained by APC-Anti-mouse anti-CD11c, FITC-Anti-mouse anti-CD40, and PE-Anti-mouse Anti-CD80 (Biolegend, USA) for 30 min at 4°C. Thereafter, DCs uptake capability was assessed by BD Accuri C6 Flowcytometer (Biosciences, USA). On the other hand, to ensure activation status of DC loaded tumor lysate, on the 6<sup>th</sup> day DCs were co-cultured with TL, as described before for 24 hours and then total RNA was extracted by TRizol (Ambion, USA). Consequently, 500 ng/ul of RNA/sample was mixed with 4 ul of 5x All- In- one RT master mix (Abm, USA), and then final volume was completed to 20 ul. After that, RNA was reversed by reverse transcriptase to cDNA (incubate 25°C for 10 min, then worm 42°C for 30 min. Thereafter, reaction was stopped at 85°C for 5 min and chilled at 4°C) by thermo cycler (ThermoFisher scientific, Finland). Later, cDNA samples were amplified by light cycler 480 II qPCR (Roche, USA) with 2x SYBR Green qPCR master mix (Bimake, China), CD11c (Itgax), MHCII (H2-Ab1), CD80, CD40 primers (Anhui, China), and *cyc* positive control gene which listed in the Table 1. Then gene expression was calculated according to *cyc* gene ct.

**Determination of T cell activation time point under TL effect.** C57BL/6 black mice were immunized by TL, and then splenocytes were harvested to separate T lymphocytes according to density. Then separated lymphocytes were co-culture with TL for 3, 6, 9, 12, 18, and 24 hours in the presence of Brefeldin A (BFA) 1,000x (Biolegend, USA) in comparison to ConA, and PBS. Next lymphocytes were collected, washed and stained (surface and intracellular) as described by Wei Ye *et al.*<sup>40</sup>, by using Pcp-Anti-mouse anti-CD3, FITC-anti-CD4, and PE- anti-CD8 for 30 min on ice. After fixation and permeabilization intracellular staining was performed by APC-anti-INF- $\gamma$  for 30 min on ice. Finally cells were assessed by BD Accuri C6 Flowcytometer. Further confirmation test of specific time points were performed by RT-qPCR. However, total RNA of lymphocytes-TL exposed was extracted by TRizol, and then RNA transcriptase was performed to get cDNA as described before, then it used to determine relative INF- $\gamma$  mRNA according to forward and reverse primers (Anhui, China) listed in the Table 2.

**Immunization and In Vivo Tumor Evaluation.** Black C57BL/6 mice were divided 7 groups ( $n = 6$ ). They were subcutaneously challenged on the right flank by  $1 \times 10^5$  Pan02 cell line. 6 days later, 1-MT was orally administered (2 mg/ml)/mouse interval 2days, as described by several protocols<sup>24,31,41</sup> to the first three group's 1-MT, 1-MT+TL+ALU, and 1-MT+DC-TL+ALU. Other groups TL+ALU, TL, ALU, and PBS were treated without 1-MT. However, mice were immunized three times subcutaneously with tumor lysate (100 ng/ml) that was mixed with adjuvant (Al(OH)<sub>3</sub> aluminum hydroxide gel). This mixture was connected with Polyethylenimine (PEI 5 mg/ml) particles. Then it was kept at 4°C for 30 min, thereafter, it was subcutaneously injected into mice.

Gene	NCBI Gene ID	Orientation	Primer sequence (5'→3')	Amplicon Size
Cd11c/Ilgax	16411	Forward	CTGGATAGCCTTCTTCTGCTG	113
		Reverse	GCACACTGTGCCGAATCA	
MHCII/H2-Ab1	14961	Forward	AGCCCCATCACTGTGGAGT	66
		Reverse	GATGCCGCTCAAACATCTGC	
CD40	21939	Forward	TGTCATCTGTGAAAAGGTGGTC	120
		Reverse	ACTGGAGCAGCGGTGTATG	
CD80	12519	Forward	ACCCCAACATAACTGAGTCT	102
		Reverse	TTCCAACCAAGAGAAGCGAGG	
Cdk1	12534	Forward	AGAAGGTACTTACGGTGTGGT	128
		Reverse	GAGAGATTCCCGAATTGCAGT	

**Table 1.** Characterization of DCs Primers used for RT-qPCR.

Gene	NCBI Gene ID	Orientation	Primer sequence (5'→3')	Amplicon Size
Ifng	15978	Forward	ATGAACGCTACACTGCATC	182
		Reverse	CCATCCTTTTGCCAGTTCCTC	
Prom1	19126	Forward	CTCCCATCAGTGGATAGAGAACT	81
		Reverse	ATACCCCTTTTGACGAGGCT	
Cd274	60533	Forward	GCTCCAAAGGACTGTACGTG	238
		Reverse	TGATCTGAAGGGCAGCATTTC	
Gapdh	14433	Forward	AGGTCGGTGTGAACGGATTG	123
		Reverse	TGTAGACCATGTAGTTGAGGTCA	

**Table 2.** Characterization of Tumor Markers Primers Used for RT-qPCR.

During the immunization programme, tumor size of all mice groups was daily measured. Thereabout, mice survival rate of another 7 groups was daily noted until the death of last mouse. However, tested groups were sacrificed and their tumor tissues, blood, spleens and draining lymph nodes were collected.

**Tumor Infiltrating Lymphocytes (TIL) and HE staining.** To investigate tumor necrosis and tumor infiltrating T lymphocytes CD4<sup>+</sup>CD25<sup>-</sup> in comparison to CD4<sup>+</sup>FOXP3<sup>+</sup>, tumor samples were sectioned 4 μm and introduced to Haematoxylin and Eosin (H&E) staining protocol according to Fischer *et al.*<sup>42</sup>. Thereafter, results were numbered and sent to a pathologist for consultation without any details about the treated and untreated tissues. Finally, tumor tissues were visualized by light microscope 200x. Furthermore, samples of each fresh enucleated tumor were mechanically digested to get single cell suspension. Next cells were counted and recruited to surface and intracellular staining. Briefly, 1 × 10<sup>6</sup> cells of tumor tissue/sample was firstly stained by Percp-anti-mouse Anti-CD3, FITC-Anti-CD4, and PE-Anti-CD25 for 30 min on ice. Then cells were fixed, permeabilized and stained by APC-Anti-FoxP3 for 30 min on ice. Finally cells were assessed by BD Accuri C6 Flowcytometer.

**Picro Sirius Red Staining.** To evaluate the impact of 1-MT and 1-MT+TL on tumor fibrosis, sections of enucleated tumor tissues were deparaffinized, rehydrated and processed for Sirius red staining as described by Segnani *et al.*<sup>43</sup>. Briefly, fixed slides were co-incubated with 0.1% Sirius red aqueous dye solution (Abcam, USA) for 1 hour. Then slides were washed in acidified water. Later it was dehydrated and mounted with DPX. Collagen red fibers and fibers area were measured by Image-pro plus 6.0 (Media Cybernetics, Inc., Rockville, MD, USA).

**Immunohistochemistry analysis of cleaved caspase-3 pathway.** To assess an impact of 1-MT and 1-MT+TL on tumor apoptosis potency, fixed tumors were deparaffinized and rehydrated by ethanol, endogenous peroxidase activity was blocked by soaking in absolute methanol including 0.3% H<sub>2</sub>O<sub>2</sub> for 30 min. then antigen was retrieved by using 10 mmol/L Tris-HCl buffer (pH 8.0) containing 1 mmol/L EDTA. Later it was blocked with normal goat serum for 5 min. Thereafter, anti-activated caspase3 antibody which was diluted 1:20 (Cell signaling, USA) was performed for overnight. Next tissues were washed by TBS and incubated with goat anti-rabbit IgG conjugated with rhodamine for 30 min. Finally they were visualized by light microscope at 200x magnification.

**Determination of cancer stem cells (CSC) viability in treated and non-treated tumor tissues.** Single cell suspensions were utilized to determine viability of CSC population in 1-MT treated and non-treated groups. However, 1 × 10<sup>6</sup> tumor cells were washed and stained by APC-Anti-mouse Anti-CD133 for 30 min on ice, and then stained cells of all groups were tested by BD Accuri C6. To confirm these results, tumor CD133 gene expression was assessed by RT-qPCR according to purchased primers (Anhui, China) listed in the Table 2 as described before.

Gene	NCBI Gene ID	Orientation	Primer sequence (5'→3')	Amplicon Size
Ccl2	20296	Forward	TTAAAAACCTGGATCGGAACCAA	121
		Reverse	GCATTAGCTTCAGATTACGGGT	
Ccl5	20304	Forward	GCTGCTTTCCTACCTCTCC	104
		Reverse	TCGAGTGACAAACACGACTGC	
Ccl7	20306	Forward	GCTGCTTTCAGCATCCAAGTG	135
		Reverse	CCAGGGACACCGACTACTG	
Ccl20	20297	Forward	GCCTCTCGTACATACAGACGC	146
		Reverse	CCAGTTCTGCTTGGATCAGC	
Tgfb1	21812	Forward	TCTGCATTGCACTTATGCTGA	100
		Reverse	AAAGGGCGATCTAGTGATGGA	
Ido1	15930	Forward	GCTTGTCTTACCACATCCAC	170
		Reverse	CAGGCGCTGTAACCTGTGT	
Il12b	16160	Forward	TGGTTTGCCATCGTTTTGCTG	123
		Reverse	ACAGGTGAGGTTCACTGTTTCT	
Il10	16153	Forward	GCTCTTACTGACTGGCATGAG	105
		Reverse	CGCAGCTCTAGGAGCATGTG	
Il6	16193	Forward	TAGTCCTTCTACCCCAATTTC	76
		Reverse	TTGGTCCTTAGCCACTCCTTC	
Il4	16189	Forward	GGTCTCAACCCCGACTAGT	102
		Reverse	GCCGATGATCTCTCAAGTGAT	

**Table 3.** Primers of Splenocytes and Tumor Cytokines used for RT-qPCR.

### Genetic expression profile of intra tumor microenvironment cytokines and pathways.

Collected tumor tissues were digested to obtain total RNA for screening CCL2 (MCP-1), CCL5 (RANTES), CCL7 (MCP-3), CCL20 (MIP3A), TGF- $\beta$ , IDO, PDL-1, TRAF1, IKK $\alpha$ , IKK $\beta$  and  $\beta$ -Catenin genes expression by the same method described above. All used primers (Anhui, China) were listed in the Table 3.

**Analysis of tumor microenvironments' signaling pathways by western blot.** First, red blood cells were disrupted, and then tumor cells were washed and fractured by using RIPA buffer (Thermo fisher, USA) with phenyl methyl sulfonyl fluoride (PMSF) a proteinase inhibitor (Sigma, USA) according to the manufacturer instructions. Total protein was assessed by BCA to determine protein concentration for every sample. Thereafter, 5  $\mu$ g/ml of each protein sample was utilized to test TGF- $\beta$ , IDO, PDL-1, CD133, NF- $\kappa$ Bp65, and  $\beta$ -Catenin pathways expression by western blot. Briefly, samples were run on 10% gel, and then transfer on blotting membrane for 30 min by Trans-blot Turbo (Bio-Rad, Singapore). After milk blocking, membranes were incubated with primary antibodies Anti-TGF- $\beta$  (Abcam, USA), Anti-IDO (Biologend, USA), Anti-PDL-1, Anti-NF- $\kappa$ Bp65 (Abcam, USA), Anti-CD133 (Boster, China), and Anti- $\beta$ -Catenin (Affinity, USA) for overnight on shaker, and then washed three times and incubated with goat anti-rabbit secondary antibody (Abcam, USA) for 1–2 hours. Finally, results visualized by gel imaging system 5200 (Tanon, China).

**Immunofluorescence imaging of tumor NF- $\kappa$ Bp65 pathway with/without 1-MT.** As described by Katsori *et al.*<sup>44</sup>, NF- $\kappa$ Bp65 signaling pathway was determined in murine pancreatic cancer cell line (Pan02) under the effect of 1-MT or without 1-MT. briefly, Pan02 cells were cultured in RPMI 1640 (Key GEN Bio, China) supplemented by 10% Fetal Bovine Serum (Hycone, Australia), and 1% penicillin and streptomycin (Gibco, USA) for 24 hours. Then  $1 \times 10^4$  cells co-cultured with/without 10 ng/ml of 1-MT. 24 hours later cells were washed with phosphate-buffered saline (PBS) then cells fixed and permeabilized by 4% formaldehyde in PBS. Next cells were blocked in 5% milk–10%, Triton X-100 in PBS for 1 h at room temperature. Then p65 visualized by purified Anti-NF- $\kappa$ Bp65 (ab32536) at 1:100 dilutions for 12 hours. After that cells were washed and probed by 1:500 dilution of Alexa Fluor 488 goat anti rabbit IgG for 2 hours. Later, DAPI nuclear counterstain was performed for 10 min. Finally, cells were washed by PBS and scanned by laser confocal microscopy FV1000-ASW (Olympus, Japan).

**Intracellular kinetics of splenic CD4<sup>+</sup> and CD8<sup>+</sup> T Cells.** Splenocytes and draining lymph nodes DLN of the 7 immunized groups were used to investigate intracellular kinetics by determination of T CD4<sup>+</sup> INF- $\gamma$ <sup>+</sup>, and CTL<sup>+</sup> INF- $\gamma$ <sup>+</sup> cells. However, lymphocytes were stained for surface markers and intracellular for INF- $\gamma$  as described above. Harvested results were presented by graph pad software. Thereafter, all CD3<sup>+</sup>CD4<sup>+</sup> and CD3<sup>+</sup>CD8<sup>+</sup> cells were collected in separate tubes by FACS Area Flowcytometer. These collected cells were fractured by TRizol to collect total RNA, which used to prepare cDNA by which expression of lymphocytes intracellular cytokines was determined under the effect of 1-MT. However, genes expression of IL-12, IL-6, IL-4, TGF- $\beta$ , and IL-10 was quantitatively determined as described above with primers (Anhui, China) listed in the Table 3.

**Gene expression profile of splenocytes' TLRs signaling pathways ascribed to 1-MT.** To determine splenocytes activated signaling pathways under 1-MT effect, spleen and NLD cells were co-cultured with tumor lysate, DCs-pulsed tumor lysate, LPS, and PBS with or without 1-MT for 24 hours at 37 °C. Then total RNA

Gene	NCBI Gene ID	Orientation	Primer sequence (5'→3')	Amplicon Size
Tlr2	24088	Forward	GCAAACGCTGTTCTGCTCAG	231
		Reverse	AGGCGTCTCCCTCTATGTATT	
Tlr3	142980	Forward	GTGAGATAACAACGTAGCTGACTG	162
		Reverse	TCCTGCATCCAAGATAGCAAGT	
Tlr4	21898	Forward	ATGGCATGGCTTACACCACC	192
		Reverse	GAGGCAATTTTGTCTCCACA	
Tlr5	53791	Forward	GCAGGATCATGGCATGTCAAC	130
		Reverse	ATCTGGGTGAGGTTACAGCCT	
Tlr7	170743	Forward	CACCACCAATCTTACCCTTACC	76
		Reverse	CAGATGGTTCAGCCTACGGAA	
Tlr8	170744	Forward	GAAAACATGCCCCCTCAGTCA	109
		Reverse	CGTCACAAGGATAGCTTCTGGAA	
Tlr9	81897	Forward	ATGGTTCTCCGTCGAAGGACT	118
		Reverse	GAGGCTTCAGCTCACAGGG	

**Table 4.** Primers of TLRs Pathways used for RT-qPCR.

Gene	NCBI Gene ID	Orientation	Primer sequence (5'→3')	Amplicon Size
Myd88	17874	Forward	TCATGTTCTCCATACCCCTGGT	175
		Reverse	AAACTGCGAGTGGGGTCAG	
Traf1	22029	Forward	AGGGTGGTGAATTACAGCAA	194
		Reverse	GCAGTGTAGAAAGCTGGAGAG	
Traf6	22034	Forward	AAAGCGAGAGATTCTTCCCTG	125
		Reverse	ACTGGGACAATTCCTAGAGC	
Irak4	266632	Forward	CATACGCAACCTTAATGTGGGG	125
		Reverse	GGAAGTATTGTATCTGTCGTCG	
Jun	16476	Forward	TTCCTCCAGTCCGAGAGCG	133
		Reverse	TGAGAAGGTCCGAGTCTTGG	
Ikkb	16150	Forward	ACAGCCAGGAGATGGTACG	297
		Reverse	CAGGGTGAAGTACTGAGTACGAGAC	
Ikkkap	230233	Forward	CTGAAGTTGCATCGGACCCTG	78
		Reverse	CTCAGCTCGCAGACAGAAACA	
Stat3	20848	Forward	CAATACCATTGACCTGCCGAT	109
		Reverse	GAGCGACTCAAAGTCCCT	
Stat4	20849	Forward	TGGCAACAATTCTGCTTCAAAC	225
		Reverse	GAGGTCCCTGGATAGGCATGT	
Nfkb1	18033	Forward	ATGGCAGACGATGATCCCTAC	111
		Reverse	TGTTGACAGTGGTATTTCTGGTG	
Nfkb2	19697	Forward	AGCGCGGGACTATGACTT	121
		Reverse	GCCCGGTTATCAAAAATCGGAT	
Ctnnb1	12387	Forward	ATGGAGCCGGACAGAAAAGC	108
		Reverse	CTTGCCACTCAGGGAAGGA	

**Table 5.** Primers of Signaling Pathways used for RT-qPCR.

was obtained, thereafter TLR2, 3, 4, 5, 7, 8, and 9 relative mRNAs were assessed by RT-qPCR by the same method was mentioned above, upon the primers (Anhui, China) listed in the Table 4.

Later, tracking of splenocytes intracellular signaling motifs ascribed 1-MT activity was performed. However, genes expressions of Myd88, TRAF6, IRAK4, Ikk $\beta$ , Ikk $\alpha$ , AP-1, NF- $\kappa$ B1, NF- $\kappa$ B2, STAT3, and STAT4 were evaluated as detailed before upon the primers (Anhui, China) listed the Table 5.

**Assessment of Periphery Immunomodulations.** The obtained blood samples were separated to plasma and lymphocytes. Lymphocytes were stained (surface and intracellular) to determine Treg<sup>+</sup> cells CD4<sup>+</sup>CD25<sup>+</sup>FOXP3<sup>+</sup> and Th1 CD3<sup>+</sup>CD4<sup>+</sup>CD25<sup>-</sup> population in treated groups in comparison to PBS. First, cells were stained by Percp-Anti-CD3, FITC-Anti-CD4, and PE-Anti-CD25 (Biolegend, USA) for 30 min on ice. Then it was fixed, permeabilized and stained by Alexa Fluor 647- anti- Foxp3 (Biolegend, USA) for 30 min on ice. Finally cells were examined by BD Accuri C6. Later, plasma samples were utilized to determine periphery TGF- $\beta$  and IL-12 cytokines by ELISA kits according to manufacturer instructions (Lington Biosciences, China).

**Statistical analysis.** Statistical analysis was performed using GraphPad Prism 6.0 for at least three independent experiments. Data were analyzed by paired student's t-test and one-way analysis of variance (ANOVA). The significant difference level was set at  $p < 0.05$ .

**Data availability.** Authors declare that all data generated or analyzed during this study are included in this published article (and its Supplementary Information files). If any interest needs more details please contact corresponding editor by private email.

## References

1. Qin, X. *et al.* Role of indoleamine 2,3-dioxygenase in an inflammatory model of murine gingiva. *J. Periodontol Res.* **52**, 107–113 (2017).
2. Godinethier, J., Hanafi, L., Piccirillo, C. A. & Lapointe, R. Indoleamine 2,3-Dioxygenase Expression in Human Cancers: Clinical and Immunologic Perspectives. *Clin. Cancer Res.* **17**, 6985–6991 (2011).
3. De Lecea, M. V. *et al.* Indoleamine 2,3 dioxygenase as a prognostic and follow-up marker in melanoma. A comparative study with LDH and S100B. *J. Eur. Acad. Dermatol. Venereol.* **31**, 636–642 (2017).
4. Hou, D. Y. *et al.* Inhibition of Indoleamine 2,3-Dioxygenase in Dendritic Cells by Stereoisomers of 1-Methyl-Tryptophan Correlates with Antitumor Responses. *Cancer Res.* **67**, 792–801 (2007).
5. Frumento, G., Rotondo, R., Tonetti, M. & Ferrara, G. B. T cell proliferation is blocked by indoleamine 2,3-dioxygenase ☆. *Transplant. Proc.* **33**, 428–430 (2001).
6. Munn, D. H. *et al.* Prevention of Allogeneic Fetal Rejection by Tryptophan Catabolism. *Science* **281**, 1191–1193 (1998).
7. Miki, T. *et al.* Blockade of tryptophan catabolism prevents spontaneous tolerogenicity of liver allografts. *Transplant. Proc.* **33**, 129–130 (2001).
8. Prendergast, G. C. *et al.* Indoleamine 2,3-dioxygenase pathways of pathogenic inflammation and immune escape in cancer. *Cancer Immunol. Immunother.* **63**, 721–735 (2014).
9. Muller, A. J., Duhadaway, J. B., Donover, P. S., Santantoward, E. & Prendergast, G. C. Inhibition of indoleamine 2,3-dioxygenase, an immunoregulatory target of the cancer suppression gene Bin1, potentiates cancer chemotherapy. *Nat. Med.* **11**, 312–319 (2005).
10. Munn, D. H. & Mellor, A. L. IDO in the Tumor Microenvironment: Inflammation, Counter-Regulation, and Tolerance. *Trends in Immunology* **37**, 193–207 (2016).
11. Friberg, M. *et al.* Indoleamine 2,3-dioxygenase contributes to tumor cell evasion of T cell-mediated rejection. *Int. J. Cancer* **101**, 151–155 (2002).
12. Takikawa, O., Yoshida, R., Kido, R. & Hayaishi, O. Tryptophan degradation in mice initiated by indoleamine 2,3-dioxygenase. *J. Biol. Chem.* **261**, 3648–3653 (1986).
13. Jiang, T. *et al.* Research progress of indoleamine 2,3-dioxygenase inhibitors. *Future Medicinal Chemistry* **7**, 185–201 (2015).
14. Uyttenhove, C. *et al.* Evidence for a tumoral immune resistance mechanism based on tryptophan degradation by indoleamine 2,3-dioxygenase. *Nat. Med.* **9**, 1269–1274 (2003).
15. Barth, H. & Raghuraman, S. Persistent infectious diseases say – IDO. Role of indoleamine-2,3-dioxygenase in disease pathogenesis and implications for therapy. *Crit. Rev. Microbiol.* **40**, 360–368 (2014).
16. Baban, B. *et al.* IDO Activates Regulatory T Cells and Blocks Their Conversion into Th17-Like T Cells. *J. Immunol.* **183**, 2475–2483 (2009).
17. Beutelspacher, S. C. *et al.* Expression of Indoleamine 2,3-Dioxygenase (IDO) by Endothelial Cells: Implications for the Control of Alloresponses. *American Journal of Transplantation* **6**, 1320–1330 (2006).
18. Chen, J. Y. *et al.* Cancer/stroma interplay via cyclooxygenase-2 and indoleamine 2,3-dioxygenase promotes breast cancer progression. *Breast Cancer Research* **16**, 410–410 (2014).
19. Munn, D. H. *et al.* Expression of indoleamine 2,3-dioxygenase by plasmacytoid dendritic cells in tumor-draining lymph nodes. *J. Clin. Invest.* **114**, 280–290 (2004).
20. Braun, D., Longman, R. S. & Albert, M. L. A two-step induction of indoleamine 2,3 dioxygenase (IDO) activity during dendritic-cell maturation. *Blood* **106**, 2375–2381 (2005).
21. Moon, Y. W., Hajjar, J., Hwu, P. & Naing, A. Targeting the indoleamine 2,3-dioxygenase pathway in cancer. *Journal for ImmunoTherapy of Cancer* **3**, 51, <https://doi.org/10.1186/s40425-015-0094-9> (2015).
22. Efimov, I. *et al.* Structure and Reaction Mechanism in the Heme Dioxygenases. *Biochemistry (Mosc.)* **50**, 2717–2724 (2011).
23. Booth, E. S., Basran, J., Lee, M., Handa, S. & Raven, E. L. Substrate Oxidation by Indoleamine 2,3-Dioxygenase Evidence for a Common Reaction Mechanism. *J. Biol. Chem.* **290**, 30924–30930 (2015).
24. Li, F., Zhang, R., Li, S. & Liu, J. IDO1: An important immunotherapy target in cancer treatment. *International Immunopharmacology* **47**, 70–77, <https://doi.org/10.1016/j.intimp.2017.03.024> (2017).
25. Spranger, S. *et al.* Up-regulation of PD-L1, IDO, and T(regs) in the melanoma tumor microenvironment is driven by CD8(+) T cells. *Science Translational Medicine* **5** (2013).
26. Lenihan, D. J. Reversibility of Effectively Treated Chemotherapy-Related Heart Failure: Raising Our Awareness and a Call to Action for Cardiology. *J. Card. Fail.* **20**, 159–160, <https://doi.org/10.1016/j.cardfail.2014.01.011> (2014).
27. Carpelanholmstrom, M. *et al.* Does anyone survive pancreatic ductal adenocarcinoma? A nationwide study re-evaluating the data of the Finnish Cancer Registry. *Gut* **54**, 385–387 (2005).
28. Ploquin, A. *et al.* Prolonged Survival in a Patient with a Pancreatic Acinar Cell Carcinoma. *Case Reports in Oncology* **8**, 447–450 (2015).
29. Von Hoff, D. D. *et al.* Increased Survival in Pancreatic Cancer with nab-Paclitaxel plus Gemcitabine. *The New England Journal of Medicine* **369**, 1691–1703 (2013).
30. Novitskiy, S. V. & Moses, H. L. Turn Off the IDO: Will Clinical Trials Be Successful? *Cancer Discovery* **2**, 673–675 (2012).
31. Hanihara, M. *et al.* Synergistic antitumor effect with indoleamine 2,3-dioxygenase inhibition and temozolomide in a murine glioma model. *J. Neurosurg.* **124**, 1594–1601 (2016).
32. Vacchelli, E. *et al.* Trial watch: IDO inhibitors in cancer therapy. *OncImmunology* **3** (2014).
33. Kandalaft, L. E. *et al.* Autologous lysate-pulsed dendritic cell vaccination followed by adoptive transfer of vaccine-primed *ex vivo* co-stimulated T cells in recurrent ovarian cancer. *OncImmunology* **2** (2013).
34. Bol, K. F., Schreiber, G., Gerritsen, W. R., De Vries, I. J. M. & Figdor, C. G. Dendritic Cell-Based Immunotherapy: State of the Art and Beyond. *Clin. Cancer Res.* **22**, 1897–1906 (2016).
35. Liau, L. M. *et al.* Treatment of a glioblastoma patient by vaccination with autologous dendritic cells pulsed with allogeneic major histocompatibility complex class I-matched tumor peptides. *Neurosurgical Focus* **9**, 1–5 (2000).
36. Ou, X. *et al.* Enhancement of dendritic cell-tumor fusion vaccine potency by indoleamine-pyrrole 2,3-dioxygenase inhibitor, 1-MT. *J. Cancer Res. Clin. Oncol.* **134**, 525–533, <https://doi.org/10.1007/s00432-007-0315-9> (2008).
37. Muller, A. J. *et al.* Immunotherapeutic Suppression of Indoleamine 2,3-Dioxygenase and Tumor Growth with Ethyl Pyruvate. *Cancer Res.* **70**, 1845–1853 (2010).

38. Holtzhausen, A., Evans, K. & Hanks, B. A. Role of the Wnt- $\beta$ -catenin signaling pathway in melanoma-mediated dendritic cell tolerization. *Journal for ImmunoTherapy of Cancer* **1**, P153, <https://doi.org/10.1186/2051-1426-1-s1-p153> (2013).
39. Asavaroengchai, W., Kotera, Y. & Mulé, J. J. Tumor lysate-pulsed dendritic cells can elicit an effective antitumor immune response during early lymphoid recovery. *Proc. Natl. Acad. Sci. USA* **99**, 931–936, <https://doi.org/10.1073/pnas.022634999> (2002).
40. Ye, W. *et al.* Cross-presentation of viral antigens in dribbles leads to efficient activation of virus-specific human memory t cells. *Journal of Translational Medicine* **12**, 100–100, <https://doi.org/10.1186/1479-5876-12-100> (2014).
41. Ninomiya, S. *et al.* Tumor indoleamine 2,3-dioxygenase (IDO) inhibits CD19-CAR T cells and is downregulated by lymphodepleting drugs. *Blood* **125**, 3905–3916 (2015).
42. Fischer, A. H., Jacobson, K. A., Rose, J. & Zeller, R. Hematoxylin and Eosin Staining of Tissue and Cell Sections. *CSH Protocols* **2008**, 0–0 (2008).
43. Segnani, C. *et al.* Histochemical Detection of Collagen Fibers by Sirius Red/Fast Green Is More Sensitive than van Gieson or Sirius Red Alone in Normal and Inflamed Rat Colon. *PLOS ONE* **10**, 1–10 (2015).
44. Katsori, A. *et al.* Inhibition of the NF- $\kappa$ B Signaling Pathway by a Novel Heterocyclic Curcumin Analogue. *Molecules* **20**, 863–878 (2015).

## Acknowledgements

This work was funded by National High Technology Research and Development Program of China (863 Program, No. 2015AA020314); Supported by National Natural Science Foundation of China (Grant No. 81570696); sponsored by Qing Lan Project; Supported by grants from the '111' project (B16046); Priority Academic Program Development of Jiangsu Higher Education Institutions (PAPD).

## Author Contributions

M.A., Y.X. and L.J. designed the study, M.A. conducted all experiments. M.A. performed data analysis and manuscript writing. Finally, manuscript was revised by Y.X. & T.T. and then all authors reviewed and approved the final draft.

## Additional Information

**Supplementary information** accompanies this paper at <https://doi.org/10.1038/s41598-018-28238-8>.

**Competing Interests:** The authors declare no competing interests.

**Publisher's note:** Springer Nature remains neutral with regard to jurisdictional claims in published maps and institutional affiliations.



**Open Access** This article is licensed under a Creative Commons Attribution 4.0 International License, which permits use, sharing, adaptation, distribution and reproduction in any medium or format, as long as you give appropriate credit to the original author(s) and the source, provide a link to the Creative Commons license, and indicate if changes were made. The images or other third party material in this article are included in the article's Creative Commons license, unless indicated otherwise in a credit line to the material. If material is not included in the article's Creative Commons license and your intended use is not permitted by statutory regulation or exceeds the permitted use, you will need to obtain permission directly from the copyright holder. To view a copy of this license, visit <http://creativecommons.org/licenses/by/4.0/>.

© The Author(s) 2018